Diminished force production and mitochondrial respiratory deficits are strain-dependent myopathies of subacute limb ischemia

Cameron A. Schmidt[1,2], **Terence E. Ryan**[1,2], **Chien-Te Lin**[1,2], **Melissa M.R. Inigo**[1,2], **Tom D. Green**[1,2], **Jeffrey J. Brault**[2,3], **Espen E. Spangenburg**[1,2], and **Joseph M. McClung**[1,2]

[1]Department of Physiology, East Carolina University, Greenville, NC

[2]Diabetes and Obesity Institute, Brody School of Medicine, East Carolina University, Greenville, NC

[3]Department of Kinesiology, East Carolina University, Greenville, NC

Abstract

Objective—Reduced skeletal muscle mitochondrial function may be a contributing mechanism to the myopathy and activity based limitations that typically plague peripheral arterial disease (PAD) patients. We hypothesized that mitochondrial dysfunction, myofiber atrophy, and muscle contractile deficits are inherently determined by the genetic background of regenerating ischemic mouse skeletal muscle, similar to how patient genetics affect the distribution of disease severity with clinical PAD.

Methods—Genetically ischemia protected (C57BL/6) and susceptible (BALB/c) mice underwent either unilateral subacute hindlimb ischemia (SLI) or myotoxic injury (CTX) for 28 days. Limbs were monitored for blood flow and tissue oxygen saturation (SO_2) and tissue was collected for the assessment of histology, muscle contractile force, gene expression, mitochondrial content, and respiratory function.

Results—Despite similar tissue SO_2 and mitochondrial content between strains, BALB/c mice suffered persistent ischemic myofiber atrophy (55.3% of C57BL/6) and muscle contractile deficits (~25% of C57BL/6 across multiple stimulation frequencies). SLI also reduced BALB/c mitochondrial respiratory capacity, assessed in either isolated mitochondria (58.3% of C57BL/6 at SLI d7, 59.1% of C57BL/6 at SLI d28 across multiple conditions) or permeabilized myofibers (38.9% of C57BL/6 at SLI d7, 76.2% of C57BL/6 at SLI d28 across multiple conditions). SLI also resulted in decreased calcium retention capacity (56.0% of C57BL/6) in BALB/c mitochondria.

Disclosures

No competing interests declared

Non-ischemic CTX injury revealed similar recovery of myofiber area, contractile force, mitochondrial respiratory capacity and calcium retention between strains.

Conclusions—Ischemia susceptible BALB/c mice suffered persistent muscle atrophy, impaired muscle function, and mitochondrial respiratory deficits during SLI. Interestingly, parental strain susceptibility to myopathy appears specific to regenerative insults including an ischemic component. Our findings indicate that the functional deficits that plague PAD patients could include mitochondrial respiratory deficits genetically inherent to the regenerating muscle myofibers.

Introduction

The recent identification of differences in the clinical course of intermittent claudication (IC, pain with exertion that is relieved with rest) and critical limb ischemia (CLI, pain at rest with or without tissue necrosis or gangrene) raise the intriguing possibility that these represent genetically determined and distinct phenotypic manifestations of peripheral arterial disease (PAD) [1–7]. Pre-clinically, different inbred mouse strains have dramatically different responses to a murine model of limb ischemia, analogous to the range of responses seen in human patients. For example, BALB/c mice demonstrate substantial muscle necrosis after both sub-acute and acute models of ischemia similar to the myopathy observed in patients with CLI, whereas C57BL/6J mice are recover rapidly from ischemia without substantial tissue loss or myopathy[3, 8–10]. Genetic haplotype analysis in these mice identified a quantitative trait locus associated with tissue necrosis that contained 37 genes with no known role in vascular biology[3]. The findings from these studies implies genetic susceptibility to limb ischemia may be a key factor in the pathology of PAD/CLI. The possibility of genetic regulation of ischemic limb pathology is further highlighted by the underwhelming results of angiogenic/neovascularization clinical trials[11] in PAD patients.

Patients with PAD, in addition to vascular defects, have altered muscle metabolism, mitochondrial respiration, expression of mitochondrial enzymes, increased oxidative stress, and somatic mutations in mitochondrial genes[12–18]. This implies that reduced skeletal muscle mitochondrial function may be a contributing mechanism to the myopathy and activity based limitations that typically plague these patients. We hypothesized that mitochondrial dysfunction, myofiber atrophy, and contractile deficits are inherently determined by the genetic background of the murine regenerating ischemic skeletal muscle. Our findings indicated that myopathy associated with subacute ischemia uniquely involves mitochondrial functional abnormalities that parallel deficits in muscle function and regeneration. While the functional deficits that plague PAD patients may be initially caused by occlusive obstruction of blood flow to the limb, the inability to recover muscle mass and function may involve analogous mitochondrial respiratory deficits genetically inherent to the muscle myofibers.

Materials and Methods

Detailed information can be found in Appendix I. Supplemental Material.

Animals

Experiments were conducted on adult (12–16 week) C57BL/6J (N=33) or BALB/cJ (N=36) mice. All work was approved by the Institutional Review Committee of East Carolina University and complied with the *Guide for the Care and Use of Laboratory Animals*, Institute of Laboratory Animal Resources, Commission on Life Sciences, National Research Council. Washington: National Academy Press, 1996. Sub-acute ischemia was performed as previously described[10]. The cardiotoxin model (CTX) of mouse muscle regeneration was performed as previously described[19] using intramuscular injections of *Naja nigricollis* venom.

Assessment of limb perfusion and tissue SO$_2$

Limb blood flow was measured using laser Doppler perfusion (LDPI) imaging as previously described[10]. Tissue oxygen saturation (SO$_2$) was assessed using a Moor VMS-OXY white light spectrometer with a CPT-300 optical probe.

Immunofluorescence (IF) and Histological Analysis

Skeletal muscle morphology, lipid and collagen deposition, vessel density, and muscle myofiber phenotype were assessed by standard light microscopy and IF microscopyMuscle regeneration was assessed on 40X tiled H&E images using an Aperio CS2 digital slide analyzer (Leica Biosystems). Lipid droplet content was assessed using oil red o counterstained in Mayer's hematoxylin, as well as IF for dystrophin and BODIPY 493/503 (Thermo Fisher).. Collagen deposition was visualized by staining in Weigert's hematoxylin solution and picrosirius red. Vascular density was assessed by IF as previously described [10, 20] and is presented as the mean CD31$^+$ area per 20X field of view. Muscle fiber typing was performed as previously described[21] using IF and presented as a proportion of total myofibers of each fiber type (MHC type IIa, MHC type IIb, or MHC type IIx).

Immunoblotting

Western blotting was performed using standard methods. Blots were visualized with chemiluminescence using standard film procedures.

Preparation of isolated skeletal muscle mitochondria for respirometry

Skeletal muscle mitochondria were isolated from the gastrocnemius, plantaris, and soleus muscles as described[22]. High-resolution O$_2$ consumption measurements were conducted using the OROBOROS O2K Oxygraph. The rate of respiration was expressed as pmol/s/mg mitochondrial protein.

Preparation of permeabilized muscle fibers for myofiber respiration

A portion of the red gastrocnemius muscle was removed and fiber bundles were separated along their longitudinal axis as previously described[23]. The rate of respiration was normalized to the myofiber dry weight and expressed as pmol/s/mg dry weight.

Mitochondrial calcium retention capacity

Changes in extramitochondrial calcium concentration were monitored fluorometrically using Calcium Green (1 μM, excitation/emission 506/532 nm, Invitrogen) as per manufacturer's instructions.

Citrate synthase activity assays

Activity assays were performed using a citrate synthase activity assay kit (Sigma) as per manufacturer's instructions.

Muscle contractile force measurements

Contractile force measurements were performed using isolated EDL muscles as previously described [24].

Total RNA and qRT-PCR Gene Expression

Total RNA was extracted from mouse EDL muscles using TRIzol (Invitrogen) and reverse-transcribed using SuperScript IV (Invitrogen). QRT-PCR was performed using an ABI ViiA-7 system (Applied Biosystems).

Statistics

Data are presented as a ratio of the ischemic (L) to the non-ischemic (R) limb, mean ± SEM. Force frequency and fiber phenotype data are presented as ischemic (L) and non-ischemic (R) limbs for each strain, mean ± SEM. Statistical analyses were carried out using StatPlus:mac (v. 2009), Vassarstats (www.vassarstats.net) or Prism 6 (v. 6.0d) software. *a priori* two sided t-tests were performed to determine mean differences in the control limbs of the strains. All other data were compared using Student's 2-tailed *t*-test or ANOVA with Holm-Sidak multiple comparison tests when applicable. In all cases, *P*<0.05 was considered statistically significant.

Results

Strain dependent myopathy during subacute ischemia

To examine the functional outcomes of ischemic myopathy, we subjected genetically ischemia resistant (C57BL/6) and ischemia susceptible (BALB/c) mice to SLI for 7- and 28-days. Similar to our previous findings[10], SLI resulted in large pockets of anucleate necrotic myofibers (SFigure 1A,B), fewer centralized nuclei and reduced total myofiber count (SFigure 1C) in BALB/c muscle as compared to C57BL/6. Myofiber size (CSA) was significantly (*P*=0.007) attenuated in BALB/c TA muscle (Figure 1A) after 28d SLI, indicating atrophy associated with ischemic regeneration unique to this parental strain. BALB/c myofiber atrophy (CSA) was driven primarily by a decrease in myofiber size in the ischemic limb ($1258.0\pm185.9\mu m^2$) and not increases in myofiber size of the contralateral control limb ($2299.4\pm172.4\mu m^2$) relative to the C57BL/6 ischemic ($2345.6\pm209.7\mu m^2$) and control ($2362.2\pm124.8\mu m^2$) limbs, respectively. QRT-PCR revealed differential patterns of expression in MAFBx (SFigure 2A), MDFI (SFigure 2B), and MuRF-1 (SFigure 2C) mRNA between the strains after SLI. *A priori* analysis revealed an increase in force generation in

the BALB/c control (R) EDL compared to the C57BL/6 (P<0.05, 40Hz-120Hz) after SLI. Specific force was uniquely decreased (P<0.05) from the contralateral control limb (R) in the BALB/c ischemic (L) limb across multiple frequencies (40Hz-120Hz; Figure 1B) and was similarly decreased (P<0.05) from the C57BL/6 ischemic (L) limb at multiple frequencies (20Hz-120Hz). Fiber typing (Figure 1C) demonstrated that BALB/c (R) EDL muscle possesses a slightly lower proportion of Type IIb (P=0.009) and greater proportion of Type IIx (P=0.01) than C57BL/6 (R) after SLI. Distributions of MyHC Type in the ischemic limb (L) were not significantly altered by SLI in either strain (Figure 1D). MHC type I was detected similarly between the strains at a proportion of less than 1%.

TA muscles were stained with picrosirius red (PR) dye and imaged using a polarized light microscope (SFigure 3A). The birefringent properties of the PR dye lead to a color hue shift from green to yellow to orange to red with increasing thickness of the collagen molecules present in the tissue. Thin collagen trended towards increase (P=0.06) after 7d SLI in BALB/c limbs (SFigure 3B) but was resolved by 28d. Thick collagen deposition was not altered between the strains at either 7d or 28d SLI (SFigure 3C). Similar to our previously reported findings for SLI[10], capillary density (CD31$^+$ area; SFigure 3D) was altered correspondingly between strains after SLI (SFigure 3E). Oil Red-O staining was performed to identify muscle lipid accumulation (SFigure 4A), which was not different between the strains at 7d SLI, but trended (P=0.09) towards an increase in BALB/c muscle (SFigure 4B). We verified differential intermuscular lipid deposition at 28d SLI with BODIPY(493/503) (SFigure 4C). BODIPY$^+$ (493/503) inclusions were not statistically different between the strains after 28d SLI (SFigure 4D).

The innate and adaptive immune responses to injury are known to differ among inbred strains of mice[25, 26]. We have previously characterized increased macrophage (CD11b$^+$) cell infiltration in BALB/c compared to C57BL/6 mice by immunofluorescence in ischemic skeletal muscle tissue at 7 days post SLI[10]. To further investigate the role of the innate immune response to SLI we performed CD11b immunostaining on muscle tissue sections from both strains following 28d SLI (data not shown), however, we were unable to detect positive signal. To confirm the presence of CDllb$^+$ cells in SLI tissue at both time-points, we performed qualitative immunoblots in EDL lysate from both strains after 7 and 28 days of SLI (SFigure 5A,B). Positive signal was detected at 7d in both strains, but not 28d. We also sought to characterize the mRNA expression changes of the proinflammatory cytokines TNFα, IL1-β, and IL-6 of both strains in response to SLI by QRT-PCR. All three cytokines increased in both strains of mice after 7d SLI. No statistically significant differences were observed in cytokine mRNA expression between the strains at 7d SLI, though all three transcripts were acutely elevated. We observed differential patterns of expression in TNFα (SFigure 5C) and IL1-β (SFigure 5D), but not IL-6 (SFigure 5E) mRNA between the strains after 28d SLI.

Muscle mitochondrial content and respiratory functional abnormalities are strain dependent during subacute limb ischemia

We examined whether alterations in muscle mitochondrial content occur following SLI. Western blotting for mitochondrial complex proteins (Figure 2A) revealed a qualitative (7d)

decrease in Complex's I-V in BALB/c muscle, which was restored to contralateral control (R) levels by d28 SLI. Citrate synthase enzyme activity (a commonly used surrogate for mitochondrial content; Figure 2B) was reduced (P=0.04) in BALB/c limb muscle after 7d SLI, and recovered to C57BL/6 levels at d28.

Tissue oxygen saturation (SO_2), measured at the distal paw following SLI, was nearly identical between the strains at all time points measured (Figure 3A). Mitochondrial respiratory capacity under multiple substrate conditions trended towards decreased values (P<0.10 across all conditions except glutamate-malate) in ischemic BALB/c muscle mitochondria after 7d SLI (Figure 3B) and significantly decreased (P<0.01 across all conditions) at 28d SLI. To assess the sensitivity of the mitochondrial permeability transition pore (mPTP), we performed a mitochondrial calcium retention capacity assay using the fluorophore Calcium Green-5N (Figure 3C). BALB/c mitochondrial calcium retention capacity was significantly (P=0.007) decreased at 28d SLI. To circumvent potential influences of isolating mitochondria[27], we also assessed the respiratory function in saponin-permeabilized myofibers isolated from the gastrocnemius muscle. Respiratory capacity was comparatively lower at both 7d and 28d SLI in BALB/c fiber bundles (P<0.05 across all conditions, excluding glutamate-malate d28) (Figure 3D). Taken together, these data suggest that substantial skeletal muscle mitochondrial impairments exist in BALB/c limb muscle during SLI, but not C57BL/6. In both isolated mitochondria and permeabilized myofiber bundle models, it is thought that respiration is primarily driven by myofiber mitochondria. This assumption is based on the relatively low density of satellite and other interstitial cells in skeletal muscle and the low mitochondrial density of resident satellite cells[28]. Further, during the isolation process connective and fat tissues are removed either mechanically or by centrifugation.

Strain independent myopathy in non-ischemic muscle regeneration

To test the regenerative response between strains to non-ischemic muscle injury, we used intramuscular injection of cardiotoxin (CTX), which we verified as non-ischemic by laser Doppler perfusion imaging and tissue SO_2 measurements (Figure 4A,B; SFigure 6A,B). H&E staining of TA muscles from 7d and 28d CTX revealed large pockets of anucleate necrotic myofibers accompanied by extensive mononuclear cell infiltration and the presence of small basophilic myofibers (Figure 4C,D), centralized nuclei and total intact fibers (Figure 4E) in both strains. Myofiber size (CSA) was similarly altered in both strains (Figure 5A) after 28d CTX. Because CTX was not directly injected into the EDL, but EDL muscles were used for force measurements in this study, EDL and TA muscles were isolated 24hrs following CTX and visualized using H&E to confirm the extent of injury in both (SFigure 6).

Force frequency relationships in isolated EDL muscles (Figure 5B) were also unaffected by parental strain and completely recovered to contralateral control values by d28 CTX. Notably, there was no increase in force generation in the BALB/c control EDL after CTX. Fiber typing (Figure 5C) revealed that, in the absence of ischemic insult, the (R) EDL muscles of C57BL/6 and BALB/c mice possess similar distributions of MyHC (Figure 5D). After CTX, the proportion of IIb myofibers is modestly increased (P=0.03) in the injured (L)

BALB/c EDL compared to the control (R). MHC type I was detected similarly between strains in a proportion of less than 1%. Taken together, these data suggest that muscle regeneration in a model of non-ischemic myofiber injury occurs similarly between C57BL/6 and BALB/c mice.

Muscle fibrosis after CTX was analyzed using picrosirius red (PR) dye (SFigure 8A). Thin collagen was increased to a greater extent (P=0.03) in BALB/c limb muscle after 7d CTX and trended (P=0.07) towards significance at 28d CTX (SFigure 8B). Limb muscle thick collagen deposition was altered similarly in both parental strains after CTX (SFigure 8C). Capillary density (SFigure 8D) was similarly altered after CTX (SFigure 8E). Lipid accumulation (Oil Red-O staining) in BALB/c limb muscle trended towards an increase (P=0.07) from C57BL/6 at 7d CTX in BALB/c muscle but was similarly altered between the strains at 28d CTX (SFigure 9A,B). Strain specific lipid positive inclusions, assessed by BODIPY(493/503), were similarly altered after d28 CTX (SFigure 9C,D).

Muscle mitochondrial content and respiratory function are strain independent during non-ischemic regeneration

Western blotting for mitochondrial complex proteins (Figure 6A) qualitatively demonstrated varying alterations in mitochondrial Complex abundances after 7d CTX, which were stabilized at 28d CTX. Citrate synthase activity (Figure 6B) was unchanged between the parental strains after 28d CTX. Paw SO_2 was similar between the strains at all time points (Figure 7A). Mitochondrial Ca^{2+} retention capacity (Figure 7C) was altered equally between the strains after CTX. Mitochondrial respiratory capacity (high-resolution respirometry) increased (P<0.004 across ADP, SUCC, ROT, ASC/TMPD, and FCCP) in the injured BALB/c mitochondria after 7d CTX (Figure 7B), but was returned to baseline at 28d CTX. Taken together these data suggest that, in the absence of ischemia, regenerating limb muscle mitochondrial content and respiratory capacity are unaffected by parental strain.

Discussion

In this study, we found that the ability of limb muscle to regenerate from an injury that does not involve reduced limb blood flow or attenuated tissue oxygen saturation (SO_2) is parental strain independent, at least with regards to ischemia divergent C57BL/6 and BALB/c mice. Regeneration from ischemic insult, however, results in contractile force deficits that correspond with muscle wasting, delayed myofiber regeneration, and mitochondrial dysfunction genetically inherent to the limb muscles of the ischemia susceptible BALB/c parental strain. In our previous description of ameroid constrictor induced subacute limb ischemia we determined that muscle myopathy (atrophy, regenerative deficits) occurred independent of strain specific alterations in muscle vascular density[10]. Here, we demonstrate the functional, morphological, and bioenergetic consequences of strain dependent ischemic myopathy. Despite similar tissue oxygen saturation (SO_2) as C57BL/6 and a lack of tissue necrosis, the mitochondria and myofiber contractile apparatus of the BALB/c limb muscle remain dysfunctional long after the onset of the ischemic insult. While the degenerative insult may be initially caused by occlusive obstruction of blood flow to the limb, the inability to recover muscle mass and function may involve deficits genetically inherent to the

muscle myofibers. Our results also demonstrate, in a refined and subacute pre-clinical PAD model, that ischemic muscle mitochondrial respiration is uniquely affected by parental strain genetics. This finding supports the notion that the plasticity of ischemic muscle is a critical determinant of the manifestation of limb pathology and lends credence to the mitochondrion as an organelle intimately involved in the failure to recover from PAD.

Ameroid constrictors have been used in mice to more closely mimic the chronic nature of human critical limb ischemia (CLI)[29] in the absence of the rapid necrosis that occurs with HLI. We previously validated this model as both subacute in nature and insufficient in severity to cause a complete cessation of blood flow, as assessed by LDPI[10]. To verify a lack of strain dependent differences in tissue oxygen, we paralleled our LDPI data with SO_2 measurements. Light guided spectrophotometry measurements, in conjunction with flow analysis, have been used in patients with CLI before and after revascularization to provide ischemic limb SO_2 and indicate the functionality of tissue blood flow[30]. Here, SO_2 measurements provided verification of the non-ischemic nature of the CTX insult in our experiments. Importantly, paw SO_2 measurements during SLI further indicate that tissue oxygenation may not be a strain dependent limiting factor in this model of PAD. This speaks to the unique nature of SLI, which results in blood flow of at least 40%[10, 29] and SO_2 values of 60% of control in the ischemic limb. These levels appear to be sufficient to overcome any substantial differences in strain dependent vascularity (collateral vessel density)[1, 2, 7, 31] or blood flow and prevent tissue loss during SLI. They are not, however, sufficient to prevent sustained deficits in muscle function and mitochondrial respiration. This points to inherent deficits in the BALB/c muscle's response to decreased blood flow and SO_2 that result in a sustained functional deficit.

Muscle function, as measured by exercise testing, is an important indicator of morbidity and mortality in PAD patients[32–34], and alterations in muscle force production due to morphological adaptations to ischemia could have severe negative consequences for patient outcomes. The use of a genetically ischemia susceptible parental strain (BALB/c) in this work is intended to be analogous with the clinical population most susceptible to ischemic pathology (i.e. CLI patients). Previous studies have suggested that a BALB/c strain dependent impairment of the myogenic response to injury exists[35–38]. Interestingly, the injury models employed in these studies often contain a remote or local ischemic component (e.g. crush injury, tissue explants). Our CTX data could suggest that, prior to the development of occlusive limb ischemia, the lack of outward susceptibility of some patients to myopathies might not accurately predict the severity of PAD manifestation. Even in the absence of superficial tissue necrosis, BALB/c mice display significant myopathies and functional deficits when ischemia is present. Clinically, restoring flow to the ischemic limb has provided little alleviation of morbidity and mortality outcomes in CLI patients [11, 39, 40], and may be indicative of an unexplored inherent susceptibility of the limb muscle tissue of these patients to ischemia.

The maintenance of mitochondrial function in ischemic skeletal muscle is a potential major contributor to tissue pathology for two primary reasons: 1) reduced ATP generation can alter ion homeostasis and contribute to the activation of the mitochondrial permeability transition pore and initiation of apoptosis, and 2) substantial degeneration and regeneration in the

ischemic limb environment requires efficient electron transport flux to satisfy the high demand for ATP production and the efficient performance of these tasks. BALB/c limb muscle mitochondria exhibit an extreme respiratory capacity reduction (~40–60% compared with the control limb); whereas mitochondrial respiratory capacity in C57BL/6 mice is unaffected. It is conceivable that the bioenergetic demand outpaces energy production in ischemic BALB/c tissues, thus contributing to an inefficient or incomplete regenerative process. A previous study[17] demonstrated, in genetically ischemia resistant C57BL/6 mice, that chronic (12wk) limb ischemia results in significant reductions in electron transport flux and oxidative damage and histological signs of myopathy despite increased mitochondrial content. Unfortunately, the use of acute HLI makes these findings difficult to compare with the data we obtained using the SLI model. A common theme, however, is that reduced skeletal muscle mitochondrial function may be a mechanism underlying the increased susceptibility to ischemic myopathies in these mice. Little is known about the impact of parental strain genetics on the ischemic mitochondrial genome or proteome. Future studies are warranted to identify specific mitochondrial targets for which to test therapeutically pre-clinically. Mitochondria provide an attractive target for therapeutic intervention in the ischemic limb due to their density in skeletal muscle and roles in the generation and maintenance of energy and redox state[41, 42], potentially gatekeeping the function and mortality of ischemic muscle myofibers during regeneration from ischemic injury.

The findings presented here are a logical "next step" to our previous observations of a strain dependent manifestation of histological pathology during ischemia[10, 20]. Of particular interest is the ischemic context dependent nature of mitochondrial respiratory abnormalities between ischemia resistant (C57BL/6) and ischemia susceptible (BALB/c) strains of mice. No differences in mitochondrial respiration were observed between the contralateral limbs of the parental strains or after CTX injury. Ischemia, however, caused a clear segregation in electron transport flux defined by significantly impaired mitochondrial respiratory capacity in BALB/c muscle. Collectively, our results suggest that a potential component of the ischemic myopathy that occurs in the BALB/c strain is an inability to handle the bioenergetic demands of limb skeletal muscle degenerative/regenerative processes. A local ADP and oxidant rich environment devoid of properly functioning mitochondria could also perpetuate a cycle of tissue degeneration and necrosis in a manner similar to the "crippled mitochondria" phenomenon, whereby suppressed mitochondrial function and reactive oxygen species generation lead to progressive cellular damage.

Conclusion

The results of this study demonstrate that genetic background is a critical determinant of the muscle functional outcome following subacute limb ischemia. The specific combination of surgical model and inbred strains of mice utilized here allowed us to demonstrate a muscle myofiber specific mitochondrial respiratory component of ischemic myopathy that corresponds with functional deficits in muscle force production in BALB/c mice. These findings provide important insight into the genetic susceptibility of muscle force production and mitochondrial electron transport chain flux to limb ischemia, which is particularly important given the role of muscle functional measures in predicting PAD manifestation and patient outcomes. These findings could lead to novel therapies targeted directly at the

skeletal muscle myofibers of the peripheral limb, which could be used alone or in combination with reperfusion strategies to improve clinical care.

Supplementary Material

Refer to Web version on PubMed Central for supplementary material.

Acknowledgments

References

1. Chalothorn D, Clayton JA, Zhang H, Pomp D, Faber JE. Collateral density, remodeling, and VEGF-A expression differ widely between mouse strains. Physiological genomics. 2007; 30(2):179–191. [PubMed: 17426116]

2. Chalothorn D, Faber JE. Strain-dependent variation in collateral circulatory function in mouse hindlimb. Physiological genomics. 2010; 42(3):469–479. [PubMed: 20551146]

3. Dokun AO, Keum S, Hazarika S, Li Y, Lamonte GM, Wheeler F, et al. A quantitative trait locus (LSq-1) on mouse chromosome 7 is linked to the absence of tissue loss after surgical hindlimb ischemia. Circulation. 2008; 117(9):1207–1215. [PubMed: 18285563]

4. Katwal AB, Dokun AO. Peripheral arterial disease in diabetes: is there a role for genetics? Current diabetes reports. 2011; 11(3):218–225. [PubMed: 21424681]

5. Matzke S, Lepantalo M. Claudication does not always precede critical leg ischemia. Vascular medicine. 2001; 6(2):77–80. [PubMed: 11530968]

6. Wang S, Zhang H, Dai X, Sealock R, Faber JE. Genetic architecture underlying variation in extent and remodeling of the collateral circulation. Circulation research. 2010; 107(4):558–568. [PubMed: 20576932]

7. Wang S, Zhang H, Wiltshire T, Sealock R, Faber JE. Genetic dissection of the Canq1 locus governing variation in extent of the collateral circulation. PloS one. 2012; 7(3):e31910. [PubMed: 22412848]

8. Chalothorn D, Faber JE. Strain-dependent variation in collateral circulatory function in mouse hindlimb. Physiol Genomics. 2010; 42(3):469–479. [PubMed: 20551146]

9. McClung JM, McCord TJ, Keum S, Johnson S, Annex BH, Marchuk DA, et al. Skeletal muscle-specific genetic determinants contribute to the differential strain-dependent effects of hindlimb ischemia in mice. The American journal of pathology. 2012; 180(5):2156–2169. [PubMed: 22445571]

10. McClung JM, McCord TJ, Southerland K, Schmidt CA, Padgett ME, Ryan TE, et al. Subacute limb ischemia induces skeletal muscle injury in genetically susceptible mice independent of vascular density. J Vasc Surg. 2015

11. Hammer A, Steiner S. Gene therapy for therapeutic angiogenesis in peripheral arterial disease - a systematic review and meta-analysis of randomized, controlled trials. VASA Zeitschrift fur Gefasskrankheiten Journal for vascular diseases. 2013; 42(5):331–339. [PubMed: 23989068]

12. Bhat HK, Hiatt WR, Hoppel CL, Brass EP. Skeletal muscle mitochondrial DNA injury in patients with unilateral peripheral arterial disease. Circulation. 1999; 99(6):807–812. [PubMed: 9989967]

13. Brass EP, Hiatt WR. Acquired skeletal muscle metabolic myopathy in atherosclerotic peripheral arterial disease. Vasc Med. 2000; 5(1):55–59. [PubMed: 10737157]

14. Brass EP, Hiatt WR, Green S. Skeletal muscle metabolic changes in peripheral arterial disease contribute to exercise intolerance: a point-counterpoint discussion. Vascular medicine. 2004; 9(4):293–301. [PubMed: 15678622]

15. Brass EP, Wang H, Hiatt WR. Multiple skeletal muscle mitochondrial DNA deletions in patients with unilateral peripheral arterial disease. Vasc Med. 2000; 5(4):225–230. [PubMed: 11213234]

16. Pipinos II, Judge AR, Zhu Z, Selsby JT, Swanson SA, Johanning JM, et al. Mitochondrial defects and oxidative damage in patients with peripheral arterial disease. Free radical biology & medicine. 2006; 41(2):262–269. [PubMed: 16814106]

17. Pipinos II, Swanson SA, Zhu Z, Nella AA, Weiss DJ, Gutti TL, et al. Chronically ischemic mouse skeletal muscle exhibits myopathy in association with mitochondrial dysfunction and oxidative damage. American journal of physiology Regulatory, integrative and comparative physiology. 2008; 295(1):R290–R296.

18. Ryan TE, Schmidt CA, Green TD, Brown DA, Neufer PD, McClung JM. Mitochondrial Regulation of the Muscle Microenvironment in Critical Limb Ischemia. Frontiers in physiology. 2015; 6:336. [PubMed: 26635622]

19. Yan Z, Choi S, Liu X, Zhang M, Schageman JJ, Lee SY, et al. Highly coordinated gene regulation in mouse skeletal muscle regeneration. The Journal of biological chemistry. 2003; 278(10):8826–8836. [PubMed: 12477723]

20. McClung JM, McCord TJ, Keum S, Johnson S, Annex BH, Marchuk DA, et al. Skeletal muscle-specific genetic determinants contribute to the differential strain-dependent effects of hindlimb ischemia in mice. The American journal of pathology. 2012; 180(5):2156–2169. [PubMed: 22445571]

21. McClung JM, Van Gammeren D, Whidden MA, Falk DJ, Kavazis AN, Hudson MB, et al. Apocynin attenuates diaphragm oxidative stress and protease activation during prolonged mechanical ventilation. Crit Care Med. 2009; 37(4):1373–1379. [PubMed: 19242334]

22. Lark DS, Reese LR, Ryan TE, Torres MJ, Smith CD, Lin CT, et al. Protein Kinase A Governs Oxidative Phosphorylation Kinetics and Oxidant Emitting Potential at Complex I. Frontiers in physiology. 2015; 6:332. [PubMed: 26635618]

23. Perry CG, Kane DA, Lin CT, Kozy R, Cathey BL, Lark DS, et al. Inhibiting myosin-ATPase reveals a dynamic range of mitochondrial respiratory control in skeletal muscle. Biochem J. 2011; 437(2):215–222. [PubMed: 21554250]

24. Spangenburg EE, Le Roith D, Ward CW, Bodine SC. A functional insulin-like growth factor receptor is not necessary for load-induced skeletal muscle hypertrophy. J Physiol. 2008; 586(1):283–291. [PubMed: 17974583]

25. Pulendran B, Smith JL, Caspary G, Brasel K, Pettit D, Maraskovsky E, et al. Distinct dendritic cell subsets differentially regulate the class of immune response in vivo. Proceedings of the National Academy of Sciences of the United States of America. 1999; 96(3):1036–1041. [PubMed: 9927689]

26. Scalzo AA, Fitzgerald NA, Wallace CR, Gibbons AE, Smart YC, Burton RC, et al. The effect of the Cmv-1 resistance gene, which is linked to the natural killer cell gene complex, is mediated by natural killer cells. J Immunol. 1992; 149(2):581–589. [PubMed: 1378069]

27. Picard M, Taivassalo T, Ritchie D, Wright KJ, Thomas MM, Romestaing C, et al. Mitochondrial structure and function are disrupted by standard isolation methods. PloS one. 2011; 6(3):e18317. [PubMed: 21512578]

28. Almada AE, Wagers AJ. Molecular circuitry of stem cell fate in skeletal muscle regeneration, ageing and disease. Nat Rev Mol Cell Biol. 2016

29. Yang Y, Tang G, Yan J, Park B, Hoffman A, Tie G, et al. Cellular and molecular mechanism regulating blood flow recovery in acute versus gradual femoral artery occlusion are distinct in the mouse. Journal of Vascular Surgery. 2008; 48(6):1546–1558. [PubMed: 19118738]

30. Rother U, Kapust J, Lang W, Horch RE, Gefeller O, Meyer A. The Angiosome Concept Evaluated on the Basis of Microperfusion in Critical Limb Ischemia Patients-an Oxygen to See Guided Study. Microcirculation. 2015; 22(8):737–743. [PubMed: 26399939]

31. Sealock R, Zhang H, Lucitti JL, Moore SM, Faber JE. Congenic Fine-Mapping Identifies a Major Causal Locus for Variation in the Native Collateral Circulation and Ischemic Injury in Brain and Lower Extremity. Circulation Research. 2013

32. McDermott MM, Guralnik JM, Ferrucci L, Tian L, Pearce WH, Hoff F, et al. Physical activity, walking exercise, and calf skeletal muscle characteristics in patients with peripheral arterial disease. Journal of Vascular Surgery. 2007; 46(1):87–93. [PubMed: 17540532]

33. McDermott MM, Hoff F, Ferrucci L, Pearce WH, Guralnik JM, Tian L, et al. Lower extremity ischemia, calf skeletal muscle characteristics, and functional impairment in peripheral arterial disease. Journal of the American Geriatrics Society. 2007; 55(3):400–406. [PubMed: 17341243]

34. McGuigan MR, Bronks R, Newton RU, Sharman MJ, Graham JC, Cody DV, et al. Muscle fiber characteristics in patients with peripheral arterial disease. Med Sci Sports Exerc. 2001; 33(12): 2016–2021. [PubMed: 11740293]

35. Grounds MD, McGeachie JK. A comparison of muscle precursor replication in crush-injured skeletal muscle of Swiss and BALBc mice. Cell and tissue research. 1989; 255(2):385–391. [PubMed: 2924339]

36. McGeachie JK, Grounds MD. Retarded myogenic cell replication in regenerating skeletal muscles of old mice: an autoradiographic study in young and old BALBc and SJL/J mice. Cell and tissue research. 1995; 280(2):277–282. [PubMed: 7781025]

37. Mitchell CA, Grounds MD, Papadimitriou JM. The genotype of bone marrow-derived inflammatory cells does not account for differences in skeletal muscle regeneration between SJL/J and BALB/c mice. Cell and tissue research. 1995; 280(2):407–413. [PubMed: 7781037]

38. Roberts P, McGeachie JK, Grounds MD. The host environment determines strain-specific differences in the timing of skeletal muscle regeneration: cross-transplantation studies between SJL/J and BALB/c mice. Journal of anatomy. 1997; 191(Pt 4):585–594. [PubMed: 9449077]

39. Annex BH. Therapeutic angiogenesis for critical limb ischaemia. Nat Rev Cardiol. 2013; 10(7): 387–396. [PubMed: 23670612]

40. Cooke JP, Losordo DW. Modulating the vascular response to limb ischemia: angiogenic and cell therapies. Circulation research. 2015; 116(9):1561–1578. [PubMed: 25908729]

41. Karch J, Molkentin JD. Regulated Necrotic Cell Death: The Passive Aggressive Side of Bax and Bak. Circ Res. 2015; 116(11):1800–1809. [PubMed: 25999420]

42. Shirihai OS, Song M, Dorn GW 2nd. How Mitochondrial Dynamism Orchestrates Mitophagy. Circ Res. 2015; 116(11):1835–1849. [PubMed: 25999423]

Clinical Relevance

Skeletal muscle morphology and function are key predictors of clinical manifestation and outcomes in PAD. Our findings demonstrate that genetic background is a critical determinant of muscle functional deficits and mitochondrial respiration. Given the range of PAD manifestations, BALB/c mice provide a useful model for studying the role of muscle and mitochondrial respiratory functional abnormalities in determining morbidity/mortality outcomes in genetically susceptible patients. Novel therapies that directly target the muscle tissue response to limb ischemia could be used alone or in conjunction with current revascularization therapies to reduce morbidity and mortality outcomes in claudicants or patients with critical limb ischemia.
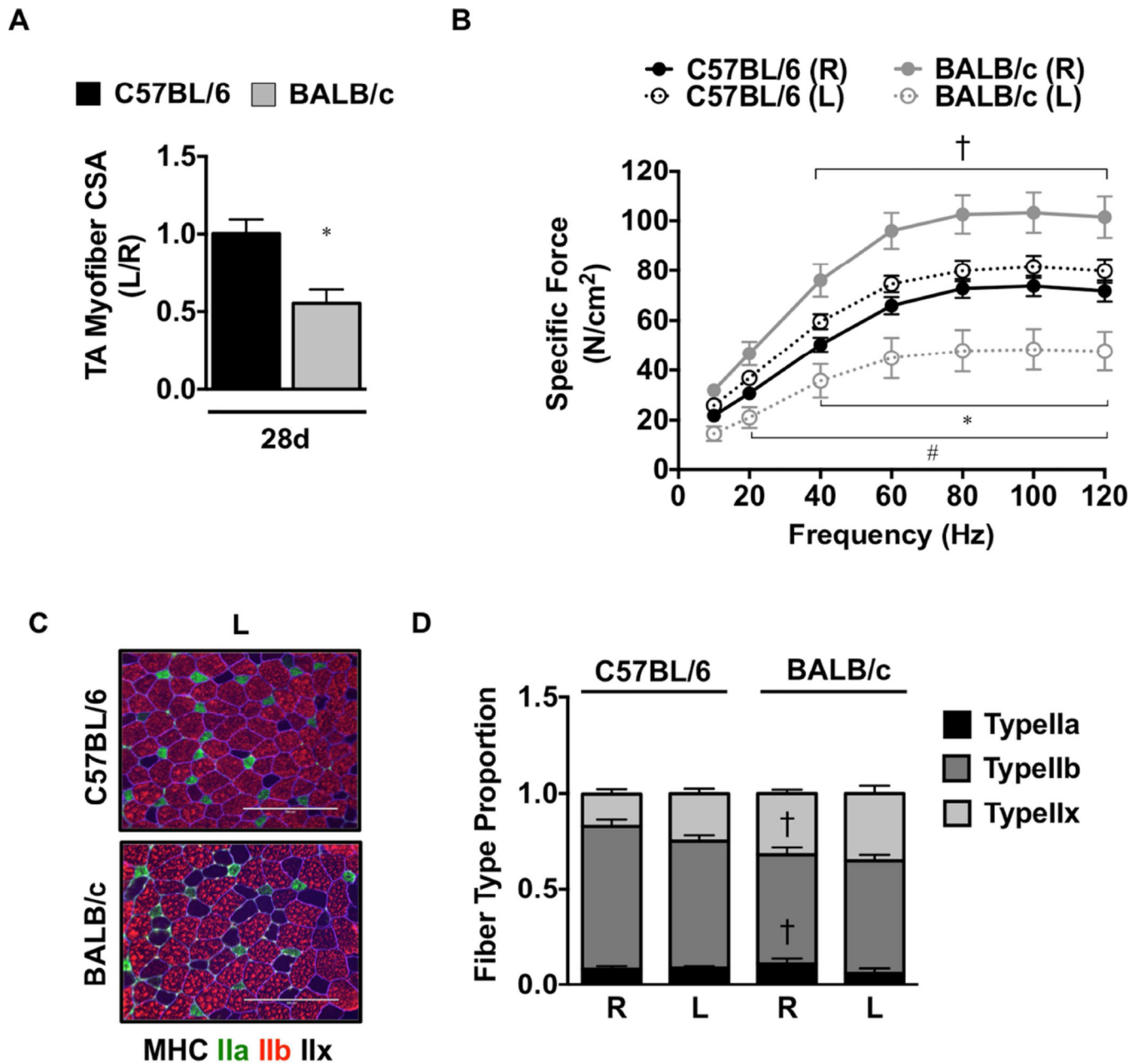
Figure 1. Muscle atrophy, morphology, and force production in ischemic hindlimbs
Sub-acute femoral artery occlusion was performed on BL6 and BALB/c mice by placement
of a single AC (1AC) on the proximal portion of the femoral artery. R, contralateral control
limb; L, ischemic limb. **A**. Sections of TA muscles were analyzed for myofiber cross
sectional area (CSA) and presented as the ratio of the ischemic (L) to the non-ischemic (R)
limb, mean ± SEM. * $P<0.05$ vs. C57BL/6. **B**. Force frequency curves were determined in
isolated EDL muscles from both strains at 28 postoperative days. * $P<0.05$ vs. day and strain
matched R. † $P<0.05$ vs. day matched C57BL/6 R. # $P<0.05$ vs. day matched C57BL/6 L. **C**.
Sections of EDL muscles were immunofluorescently labeled with selective myosin heavy
chain antibodies to determine the proportion of each fiber type (IIa, IIb, IIx) present. Scale
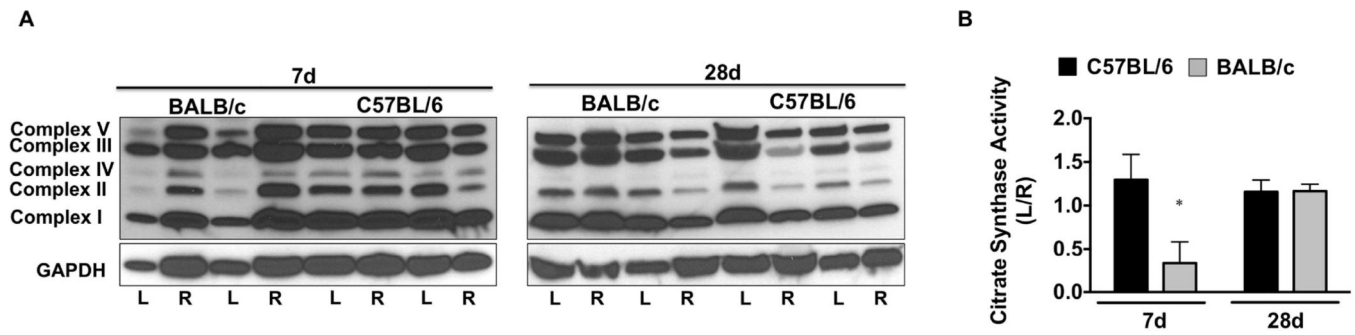
bar inlays are 200µm in length. (**D**). Myofiber phenotypes are presented as the relative proportions of each in the ischemic (L) and non-ischemic (R) limbs, mean ± SEM. † *P*<0.05 vs. C57BL/6 R. All data are representative of N 6/strain/time point.
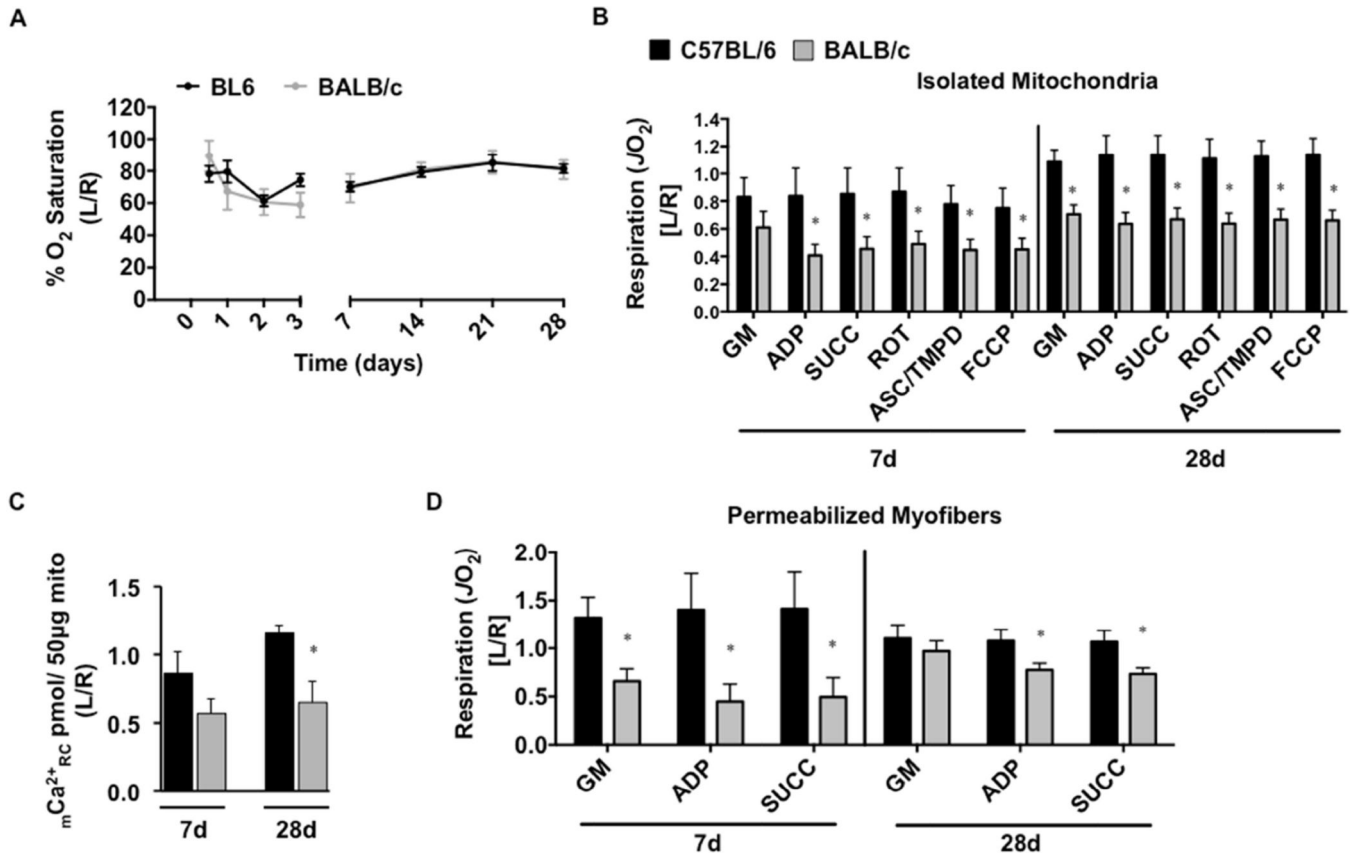
Figure 2. Parental strain effects on ischemic tissue mitochondrial content
Sub-acute femoral artery occlusion was performed on C57BL/6 and BALB/c mice by placement of a single AC (1AC) on the proximal portion of the femoral artery, immediately proximal to the epigastric arterial branch. Western blotting for mitochondrial complex content was performed for qualitative observation of complex I-V protein abundances, with GAPDH protein blotting as a loading reference (**A**). **B**. Citrate synthase activity was determined in EDL muscle as an indicator of muscle mitochondrial content. Data are representative of the ratio of the ischemic (L) to the non-ischemic (R) limb, mean ± SEM and representative of N 6/strain/time point. * P<0.05 vs. day matched C57BL/6.

Figure 3. Limb muscle mitochondrial response to sub-acute hindlimb ischemia

Sub-acute femoral artery occlusion was performed on C57BL/6 and BALB/c mice by placement of a single AC (1AC) on the proximal portion of the femoral artery, immediately proximal to the epigastric arterial branch. Paw tissue oxygen saturation (%SO$_2$), measured via white light reflectance spectroscopy, was analyzed to determine distal limb O$_2$ (**A**). **B**. Mitochondrial respiration (oxygen consumption rate-JO$_2$, as a measure of electron transport system flux) was measured in isolated mitochondria using high-resolution respirometry. The respiratory states assessed were: 1.) glutamate/malate supported state 2 respiration (GM) 2.) glutamate/malate supported state 3 (ADP) 3.) GM and succinate supported state 3 (SUCC) 4.) succinate supported state 3 (ROT) 5.) ascorbate/TMPD supported state 3 (ASC/TMPD) and 6.) FCCP supported state 3 uncoupled respiration (FCCP). **C**. Ca^{2+} reuptake was measured in ischemic (L) and control (R) mitochondria isolated from the limb plantar flexors (gastrocnemius, plantaris, and soleus) as a function of mitochondrial integrity and resistance to permeability transition. **D**. Oxygen consumption was also determined in saponin permeabilized myofiber bundles isolated from the gastrocnemius muscle. Data are representative of the ratio of the ischemic limb (L) to the untreated control limb (R). * P<0.05 vs. C57BL/6. All data are means ± SEM and representative of N 6/strain/time point.
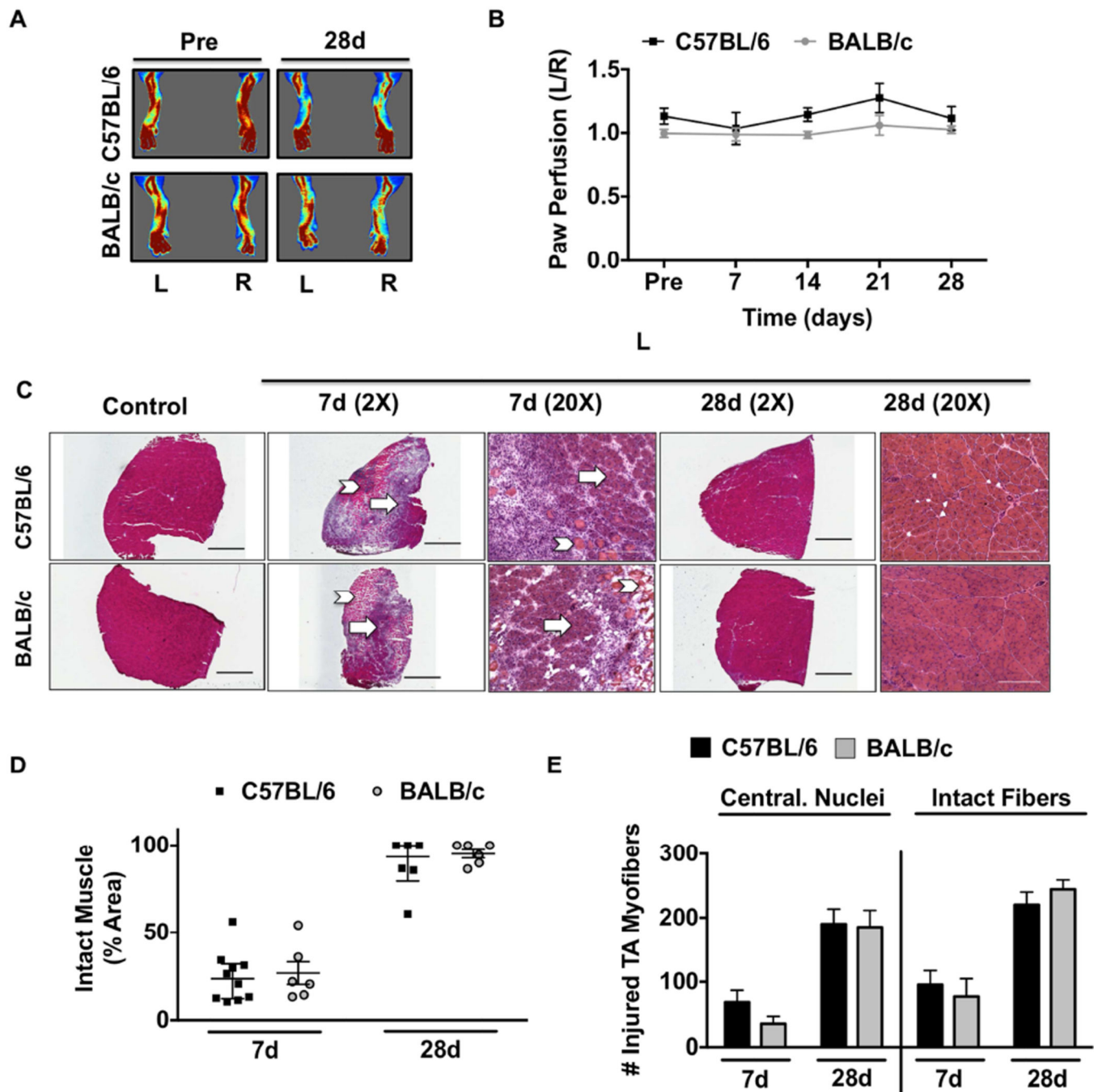
Figure 4. Strain independent myopathy with non-ischemic myotoxin injury

Cardiotoxin (CTX) was injected intramuscularly into the TA and the lateral/medial heads of the gastrocnemius muscle. A sham injection (Ctrl) of equal volume sterile saline was injected in the same muscles in the contralateral control limb (R). A. Representative laser Doppler perfusion images (LDPI) of the paw before and during recovery from cardiotoxin injection. B. Quantification of blood flow in the hind paw, presented as the ratio of the CTX injected (L) limb to the sham injected control (R) limb. C. Representative 2X and 20X images of hematoxylin and eosin (H&E) stained sections of tibialis anterior (TA) muscles 7

and 28 days after CTX (L) injury. Arrows indicate intact muscle; Chevrons indicate regions of anucleate necrotic fibers. Scale bar inlays are 1000μm in length(2X), and 200μm in length(20X). D. Muscle regeneration was quantified from 2X H&E images by measuring the total regions of interest (ROI; area) containing necrotic/anuclueate myofibers, which is represented by median and interquartile range. E. Total myofibers with centralized nuclei (Central. Nuclei) and total myofiber number (Intact Fibers) were determined in representative 10X images. All data are means ± SEM and representative of N 6/strain/time point.
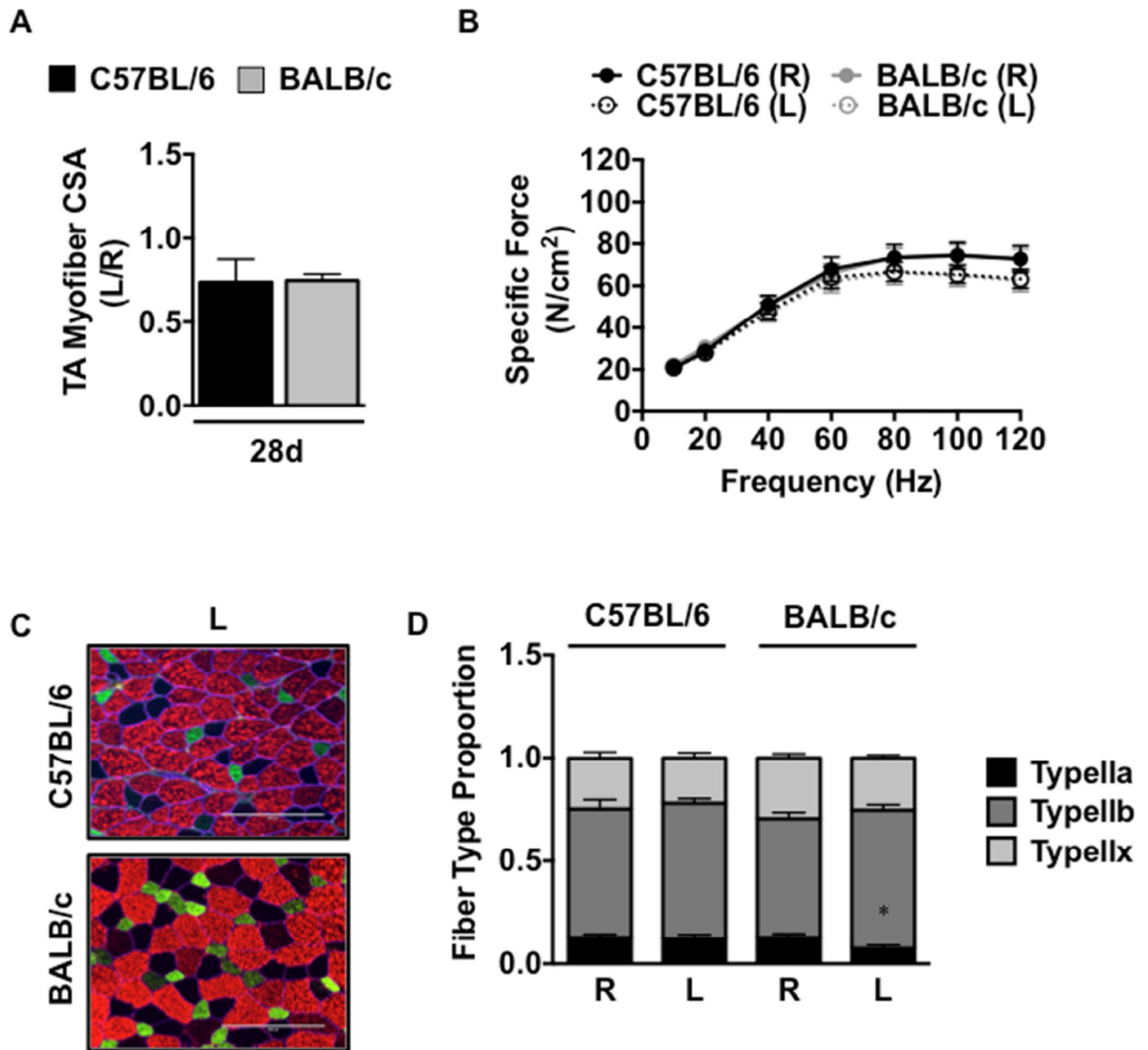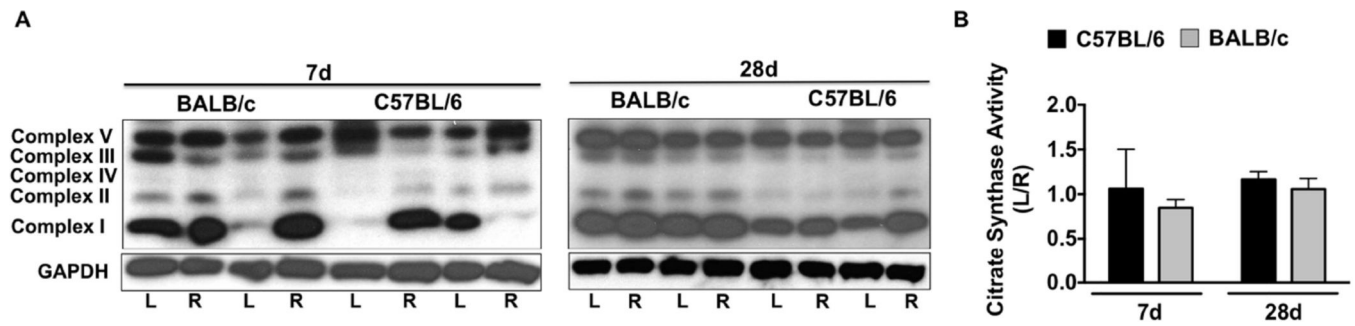
Figure 5. Muscle atrophy, morphology, and force production after a non-ischemic injury

Non-ischemic muscle regeneration was induced by cardiotoxin (CTX) injection. **A**. Sections of TA muscles were analyzed for myofiber cross sectional area (CSA) and presented as the ratio of the ischemic (L) to the non-ischemic (R) limb, mean ± SEM. **B**. Force frequency curves were determined in isolated EDL muscles from both strains at 28 postoperative days. **C**. Sections of EDL muscles were immunofluorescently labeled with selective myosin heavy chain antibodies to determine the proportion of each fiber type (IIa, IIb, IIx) present. 200μm in length(20X). (**D**). * $P<0.05$ vs. strain matched R. All data are means ± SEM and representative of N 6/strain/time point.
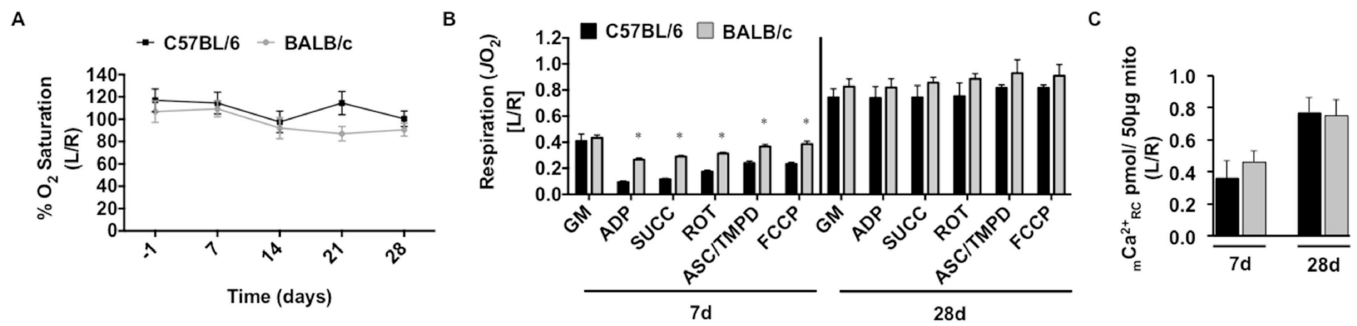
Figure 6. Muscle mitochondrial content after a non-ischemic injury
Non-ischemic muscle regeneration was induced by cardiotoxin (CTX) injection. Western blotting for mitochondrial complex content was performed for qualitative observation of complex I-V protein abundances, with GAPDH protein blotting as a loading reference (**A**). **B**. Citrate synthase activity was determined in EDL muscle as an indicator of muscle mitochondrial content. Data are representative of the ratio of the ischemic (L) to the non-ischemic (R) limb, mean ± SEM and representative of N 6/strain/time point. * *P*<0.05 vs. day matched C57BL/6.

Figure 7. Limb muscle mitochondrial response to non-ischemic injury

Non-ischemic muscle regeneration was induced by cardiotoxin (CTX) injection. Paw tissue oxygen saturation (%SO$_2$), measured via white light reflectance spectroscopy, was analyzed to determine distal limb O$_2$ (**A**). **B**. Mitochondrial respiration (oxygen consumption rate-JO$_2$, as a measure of electron transport system flux) was measured in isolated mitochondria using high-resolution respirometry. The respiratory states assessed were: 1.) glutamate/malate supported state 2 respiration (GM) 2.) glutamate/malate supported state 3 (ADP) 3.) GM and succinate supported state 3 (SUCC) 4.) succinate supported state 3 (ROT) 5.) ascorbate/TMPD supported state 3 (ASC/TMPD) and 6.) FCCP supported state 3 uncoupled respiration (FCCP). Data are representative of the ratio of the injured limb (L) to the untreated control limb (R). * P<0.05 vs. C57BL/6. **C**. Ca^{2+} reuptake was measured in injured (L) and control (R) limb mitochondria isolated from the plantar flexors (gastrocnemius, plantaris, and soleus) as a function of mitochondrial integrity and resistance to permeability transition. Data are representative of the ratio of the ischemic (L) to the non-ischemic (R) limb, mean ± SEM and representative of N 6/strain/time point. * P<0.05 vs. day matched C57BL/6.